Explaining Some Anomalies in Catalytic Activity Values in Some Zirconocene Methyl Cations: Local Hyper-Softness

1 AUTHOR:

Jorge Ignacio Martínez-Araya
Universidad Andrés Bello
**29** PUBLICATIONS **304** CITATIONS

SEE PROFILE

Explaining Some Anomalies in Catalytic Activity Values in Some Zirconocene Methyl Cations: Local Hyper-Softness

Jorge Ignacio Martínez-Araya*

Dirección de Investigación y Desarrollo/Facultad de Ingeniería, Campus Tobalaba, Sede Santiago, Universidad Pedro de Valdivia, Avda. Tobalaba 1275, Código Postal 7510275, Providencia−Santiago, Chile

Dirección de Postgrado e Investigación, Sede Providencia, Universidad Autónoma de Chile, Carlos Antúnez 1920, Código Postal 7500566, Providencia−Santiago, Chile

ABSTRACT: Some metallocene methyl cations made of zirconium, that have been used as catalysts in polymerization of ethylene, were studied by means of the conceptual density functional theory (DFT). Up to now, catalytic activity, a pure experimental parameter, that measures the kilograms of polyethylene produced per gram of metallocene, per time unit, per temperature unit, and per pressure unit, has been mainly explained in terms of steric hindrance at least qualitatively, meaning that a catalyst having a higher steric hindrance will present a lower catalytic activity. However, there has not been a satisfactory explanation for those few cases in which the steric effect cannot be linked with the catalytic activity, thus meaning that the electronic inductive effect predominates over the steric effect. As a consequence, the electronic inductive effect must be quantified through the use of a proper descriptor based on quantum chemical calculations and, in addition, this descriptor should be able to explain high values of catalytic activities even when the steric effect seems to play an unfavorable role. This work has demonstrated that a local reactivity descriptor called local hyper-softness coming from the conceptual DFT is a suitable pure theoretical parameter that explains such anomalies in some values of catalytic activity. It is expected that the findings exposed here can help to estimate catalytic activity and lead to a more rational design of new catalysts by means of computational chemistry.
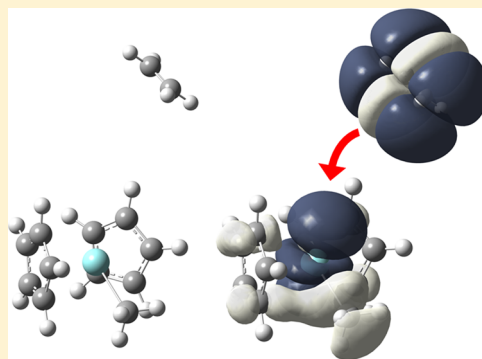
1. INTRODUCTION

A polymerization reaction catalyzed by metallocene methyl cations[1−12] of group 4 is a complex multistep process involving, essentially, three kinds of key stages: initiation, propagation, and termination steps.[13] In order to computationally simulate this process, many researchers have used the accepted Cossée−Arlman's mechanism[14−16] under the assumption that ethylene concentration is low. At high ethylene concentrations, the Ystenes' mechanism[17,18] should be used. However, for either of these mechanisms,[1,2,10,11,16] all of the theoretical and experimental evidence indicate that the major affinity for π-electrons coming from an olefin is presented by the metallic atom of the catalyst. In this way the polymerization is catalyzed through a coordination of the olefin onto the metallic atom. This implies that not only is a simple electrostatic interaction driving this type of catalytic process, but rather a covalent interaction operates predominantly and that prevents a coordination of the olefin on any site of cationic catalyst excepting on the metal center.

Although metallocene methyl cationic catalysts made of zirconium, also called zirconocene methyl cations, are often formed from neutral dichlorometallocenes of Zr by a reaction with a co-catalyst,[19−21] which is a Lewis acid that is able to replace chlorine atoms by one methyl group to produce the active species, the most famous being the methylaluminoxane

(MAO),[22] in this work the analysis has been focused on the cationic species alone without taking into account either the co-catalyst or the solvent effect because the interest is focused on the intrinsic local reactivity of these catalytic species by themselves. Experimentally, the co-catalyst is added in order to ease the formation of zirconocene methyl cation; on the contrary, if not used, the polymerization process would not occur. For the sake of simplicity, the presence of the co-catalyst has been suppressed in this work because its computational modeling is still a matter of debate[23−26] and because the co-catalyst is not an issue of interest in this work. The monomer called ethylene (an olefin) has been excluded from this work because its nature is a not a focus of attention; additionally, it is understood that its regiochemistry of insertion makes no sense in comparison, for instance, with the regiochemistry of propylene insertion,[27] so that the most relevant aspect is the local reactivity on the zirconium atom that is presented by each catalytic system, provided that ethylene is the monomer to be used. Olefins whose regiochemistry is relevant (for instance, propylene) imply an additional analysis on the orientation of

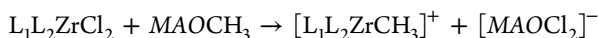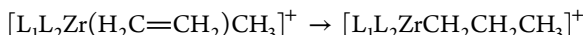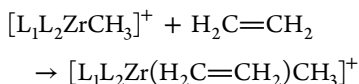the monomer when it gets closer and closer to the metallic atom of the catalyst.

Experimentally, it is well-known that the first step of the polymerization process is the catalyst activation by the co-catalyst[13,20,23] followed by the initiation stage where the reaction is divided into two elementary reaction steps: the first one consists of a coordination of one ethylene molecule on a zirconocene methyl cation, so forming a π-complex, and the second one implies a migratory insertion of the methyl group (originally linked to the metal) into the coordinated ethylene molecule. This generates a new catalytic species called zirconocene propyl cation, which preserves very similar catalytic capabilities as exhibited by the first zirconocene methyl cation so that a second ethylene after being coordinated onto the metal center is turned into a pentyl group and so on; as a consequence, with the cyclic sequence of coordination and migration, long chains of carbon atoms are produced. The reaction mechanism of this typical catalyzed polymerization process without incorporating a comonomer is given by the following scheme, where L_1 and L_2 are the aromatic ligands that are often used to produce metallocenes:
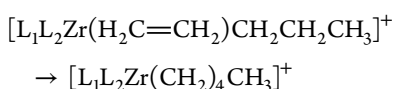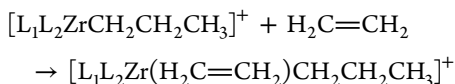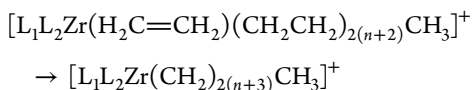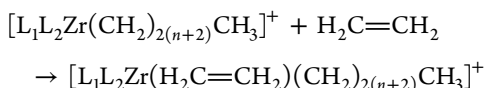
Activation

$$L_1L_2ZrCl_2 + MAOCH_3 \rightarrow [L_1L_2ZrCH_3]^+ + [MAOCl_2]^-$$

Initiation

$$[L_1L_2ZrCH_3]^+ + H_2C{=}CH_2$$
$$\rightarrow [L_1L_2Zr(H_2C{=}CH_2)CH_3]^+$$

$$[L_1L_2Zr(H_2C{=}CH_2)CH_3]^+ \rightarrow [L_1L_2ZrCH_2CH_2CH_3]^+$$

Propagation

$$[L_1L_2ZrCH_2CH_2CH_3]^+ + H_2C{=}CH_2$$
$$\rightarrow [L_1L_2Zr(H_2C{=}CH_2)CH_2CH_2CH_3]^+$$

$$[L_1L_2Zr(H_2C{=}CH_2)CH_2CH_2CH_3]^+$$
$$\rightarrow [L_1L_2Zr(CH_2)_4CH_3]^+$$

after n processes like this

$$[L_1L_2Zr(CH_2)_{2(n+2)}CH_3]^+ + H_2C{=}CH_2$$
$$\rightarrow [L_1L_2Zr(H_2C{=}CH_2)(CH_2)_{2(n+2)}CH_3]^+$$

$$[L_1L_2Zr(H_2C{=}CH_2)(CH_2CH_2)_{2(n+2)}CH_3]^+$$
$$\rightarrow [L_1L_2Zr(CH_2)_{2(n+3)}CH_3]^+$$

Termination by hydrogenolysis

$$[L_1L_2ZrCH_2(CH_2)_{2n+5}CH_3]^+ + H_2$$
$$\rightarrow [L_1L_2Zr(H_2)CH_2(CH_2)_{2n+5}CH_3]^+$$

$$[L_1L_2Zr(H_2)CH_2(CH_2)_{2n+5}CH_3]^+$$
$$\rightarrow TS$$
$$\rightarrow [L_1L_2ZrH(CH_3(CH_2)_{2n+5}CH_3)]^+$$

$$[L_1L_2ZrH(CH_3(CH_2)_{2n+5}CH_3)]^+$$
$$\rightarrow [L_1L_2ZrH]^+ + CH_3(CH_2)_{2n+5}CH_3$$
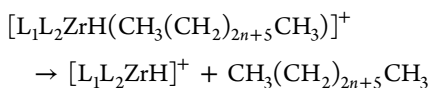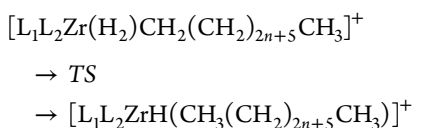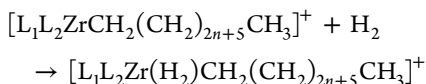
Termination by β-H transfer to the metal center

$$[L_1L_2ZrCH_2CH_2(CH_2)_{2(n+2)}CH_3]^+$$
$$\rightarrow TS$$
$$\rightarrow [L_1L_2ZrH(H_2C{=}CH(CH_2)_{2(n+2)}CH_3)]^+$$

$$[L_1L_2ZrH(H_2C{=}CH(CH_2)_{2(n+2)}CH_3)]^+$$
$$\rightarrow [L_1L_2ZrH]^+ + H_2C{=}CH(CH_2)_{2(n+2)}CH_3$$
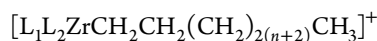
Termination by β-H transfer to monomer in the complex

$$[L_1L_2Zr(CH_2)_{2(n+3)}CH_3]^+ + H_2C{=}CH_2$$
$$\rightarrow [L_1L_2Zr(H_2C{=}CH_2)(CH_2)_{2(n+3)}CH_3]^+$$

$$[L_1L_2Zr(H_2C{=}CH_2)(CH_2)_{2(n+3)}CH_3]^+ \rightarrow TS$$

$$TS \rightarrow [L_1L_2ZrCH_2CH_3(H_2C{=}CH(CH_2)_{2(n+2)}CH_3)]^+$$

$$[L_1L_2ZrCH_2CH_3(H_2C{=}CH(CH_2)_{2(n+2)}CH_3)]^+$$
$$\rightarrow [L_1L_2ZrCH_2CH_3]^+ + H_2C{=}CH(CH_2)_{2(n+2)}CH_3$$
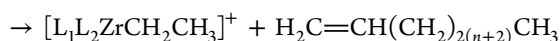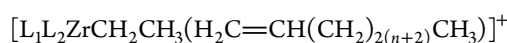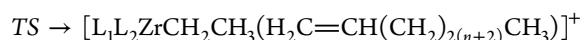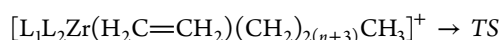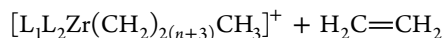
Note that an ionic pair is formed as a product during the Activation stage. However, it is assumed that both these species are separated enough to allow a coordination of monomer on the metal center o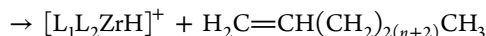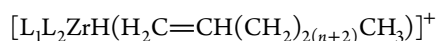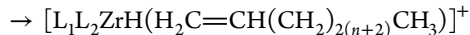f zirconocene methyl cation; for that reason, in several computational models, the presence of *MAO* and *MAOCl₂* is not taken into account, especially when the main focus of analysis is the zirconocene methyl cation. According to this accepted mechanism,[13] the computational quantum modeling of the catalyzed polymerization process is not an easy task, thus forcing a search for strategies that allow one to infer information about the catalysis process without simulating all of these steps. One of these strategies lies in analyzing one factor that appears during the whole polymerization process: Since the carbon chain varies its length and its conformation changes more and more as the carbon chain increases its size, the attention should be put on the catalyst, because it satisfies the requirement of being the same parameter even during the coordination of monomers which are inserted into an increasing carbon chain. One reason is based on the fact that the metal center is the site of coordination whose reactivity remains almost constant during the entire polymerization process. Then, a study of the reactivity of the coordination site of the catalyst makes sense.

So, if our interest is centered on looking for an approximation to the catalytic activity from the quantum chemistry point of view, according to the mechanism exposed above, the study of each stage in detail makes no sense; hence, the entire study should be oriented toward the catalyst *per se*. That is why it has been decided to concentrate the effort of study on the metal center of the catalyst, without taking into account all of these stages, because this study has been performed under the assumption that this reaction mechanism operates in all of the catalysts that have been analyzed and, as a consequence, if all of remaining experimental conditions are the same, then the difference among catalytic activities are due only to the characteristics of the respective catalyst. If one or more experimental conditions in a group of experimental results are different, the analysis is no more valid and the group of catalysts must be split into smaller subgroups in order to ensure that experimental conditions are exactly the same or very similar; so, a possible difference should be attributed to the nature of the
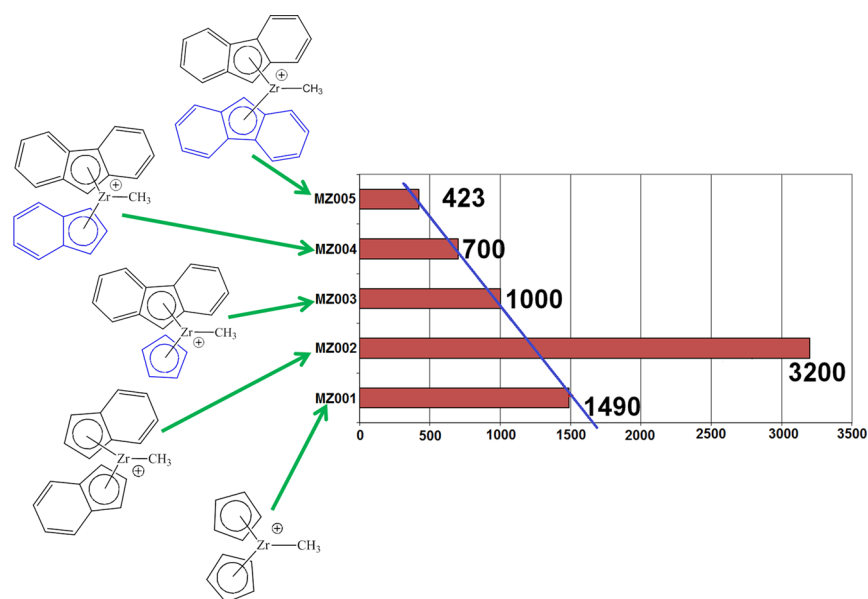
Figure 1. Values of catalytic activities of five zirconocene methyl cations: **MZ001** = bis(cyclopentadienyl)methyl zirconium cation; **MZ002** = bis(indenyl)methyl zirconium cation; **MZ003** = (fluorenyl)(cyclopentadienyl)methyl zirconium cation; **MZ004** = (fluorenyl)(indenyl)methyl zirconium cation; and **MZ005** = bis(fluorenyl)methyl zirconium cation. Experimental results (catalytic activities expressed in kilograms of polyethylene per gram of metallocene per hour and per pressure unit) come from an article written by Alt and Köppl under the following experimental conditions: the solvent is *n*-pentane and ethylene pressure is 10.0 bar. All values reported were obtained at 60 °C. Note that, according to the generally observed trend, MZ002 noticeably escapes from this behavior, thus suggesting that the steric effect does not influence on the catalytic activity value of MZ002.

respective catalyst solely, meaning the molecular structure responsible for steric and electronic inductive effects.

The coordination of ethylene and the migration of the respective alkyl group (methyl group in the case of the **Initiation** stage; propyl, pentyl, and so on in the case of the **Propagation** stage) toward the coordinated ethylene should be intuitively favored when the aromatic ligands (L_1 and L_2) linked to the metal center exhibit a low steric hindrance. As a result, the steric effect influences the entire polymerization process, and unfortunately, it is not possible to neglect this effect. Even so, under this assumption, an analysis centered over the zirconocene methyl cationic species seems to be very reasonable to explain differences among catalytic activities.

Nevertheless, in the present study a few zirconocene methyl cations have been selected from a publication written by H. G. Helmut and A. Koppl;[28] some values of catalytic activities seem to be controlled not by steric effects, but rather by electronic inductive effects. The reader can check that the cited article is an extended collection of experimental results performed under very controlled experimental conditions, so it is possible to carry out a systematic theoretical analysis to compare catalytic activities of different zirconocene systems. The numeric labeling used in this work is exactly the same as described in the aforementioned article;[28] additionally, the MZ abbreviation was employed in the present work to emphasize that metallocenes under study are made of zirconium.

In order to illustrate the relevance of the topic broached here, Figure 1 will be used as a key example. In such a picture, the catalytic activity values are depicted as horizontal bars; the zirconocene methyl cationic species imply aromatic ligands as cyclopentadienyl (Cp), indenyl (Ind), and fluorenyl (Flu), with Flu being the largest and Cp the smallest. When focusing the attention on zirconocene methyl cations MZ003, MZ004, and MZ005 (Figure 1), it is possible to distinguish that the upper

ligand is always the same (Flu), while the lower ligand is different (because it changes from Cp in MZ003 to Flu in MZ005). As a result, within this subgroup, it is possible to easily infer that the catalytic activity decreases as the size of one of the ligands increases: this is because a bulky ligand prevents or makes more difficult a coordination of ethylene on the metallic atom. So far, this is nothing new and a simple rule might be followed: the higher the steric hindrance is, the lower the catalytic activity, thus allowing us to intuitively estimate values of catalytic activity before measuring it in laboratory.

However, the same graphic (Figure 1) shows an apparent contradictory effect, because although MZ002 possesses two indenyl ligands which are bulkier than two cyclopentadienyl ligands, MZ002 presents a catalytic activity value that is greater than double the catalytic activity of MZ001. This can be interpreted as the steric effect not controlling the catalytic activity and the other effect (inductive electronic) predominating over the first one to favor the coordination of ethylene on the metal center. The reader can observe that the catalytic activities of MZ001, MZ003, MZ004, and MZ005 follow a kind of linear trend, whereas MZ002 escapes from this tendency noticeably. This work will demonstrate that a good conceptual tool to explain these deviations and measure such inductive electronic effects is the local hyper-softness.

A set of 25 zirconocene methyl cations[28] (Figures 2 and 3), that have been used in ethylene polymerization, were characterized through the use of a local reactivity descriptor called local hyper-softness in order to explain those cases where the increase of steric hindrance seems to favor the catalytic activity instead of decreasing it.

This article is schematized as follows: first, the Theoretical Background will give the reader enough information about the aforementioned descriptor of local reactivity that has been employed in this work; second, the Computational Methods
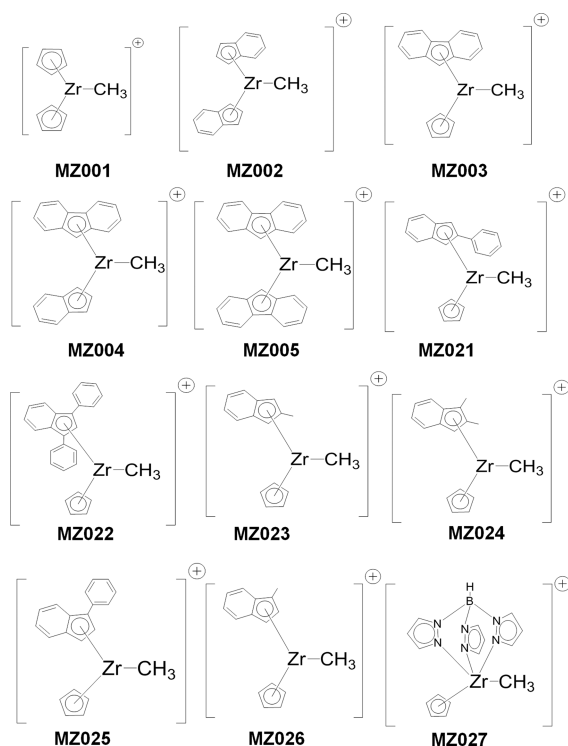
Figure 2. Subgroup A: **MZ001, MZ002, MZ003, MZ004,** and **MZ005.** Subgroup B: **MZ021** = (2-phenylindenyl)(cyclopentadienyl)methyl zirconium cation; **MZ022** = (1,3-diphenylindenyl)-(cyclopentadienyl)methyl zirconium cation; **MZ023** = (2-methylindenyl)(cyclopentadienyl)methyl zirconium cation; **MZ024** = (1,2-dimethylindenyl)(cyclopentadienyl)methyl zirconium cation; and **MZ025** = (1-phenylindenyl)(cyclopentadienyl)methyl zirconium cation. Subgroup C: **MZ001, MZ026** = (1-methylindenyl)-(cyclopentadienyl)methyl zirconium cation; **MZ027** = [tris-(pyrazolyl)borate](cyclopentadienyl)methyl zirconium cation.
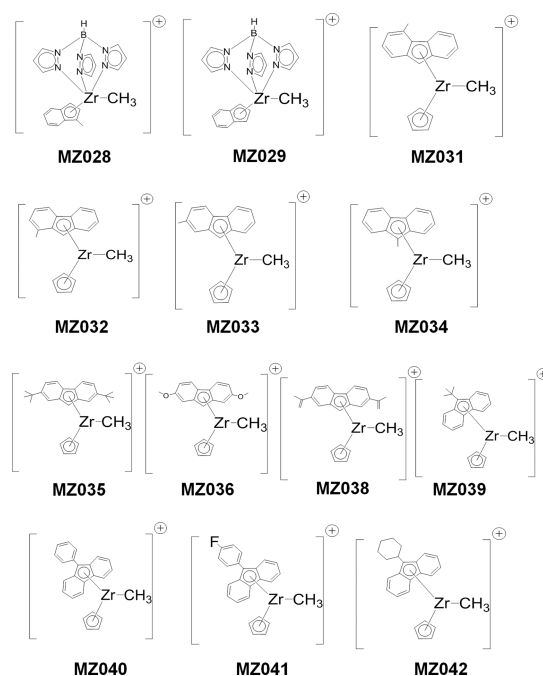

Figure 3. Continuation of Subgroup C: **MZ028** = [tris(pyrazolyl)-borate](1-methylindenyl)methyl zirconium cation and **MZ029** = [tris(pyrazolyl)borate](indenyl)methyl zirconium cation. Subgroup D: **MZ003, MZ031** = (4-methylfluorenyl)(cyclopentadienyl)methyl zirconium cation; **MZ032** = (1-methylfluorenyl)(cyclopentadienyl)-methyl zirconium cation; **MZ033** = (2-methylfluorenyl)-(cyclopentadienyl)methyl zirconium cation; and **MZ034** = (9-phenylfluorenyl)(cyclopentadienyl)methyl zirconium cation. Subgroup E: **MZ003, MZ035** = (2,7-di-*tert*-butylfluorenyl)(cyclopentadienyl)-methyl zirconium cation, **MZ036** = (2,7-dimethoxyfluorenyl)-(cyclopentadienyl)methyl zirconium cation; and **MZ038** = [2,7-di(1-methylvinyl)phenylfluorenyl](cyclopentadienyl)methyl zirconium cation. Subgroup F: **MZ003; MZ039** = (9-*tert*-butylfluorenyl)-(cyclopentadienyl)methyl zirconium cation; **MZ040** = (9-phenylfluorenyl)(cyclopentadienyl)methyl zirconium cation; **MZ041** = [9-(4-fluorophenyl)fluorenyl](cyclopentadienyl)methyl zirconium cation; and **MZ042** = (9-cyclohexylfluorenyl)(cyclopentadienyl)-methyl zirconium cation.

section indicates methodologies that have been used to obtain the condensed hyper-softness values. Third, Results and Discussion provide the critical analysis concerning this research and Conclusions are given in the last section.

2. THEORETICAL BACKGROUND: LOCAL HYPER-SOFTNESS

The noticeable capability of a zirconocene methyl cation to coordinate an olefin is due to the fact that an olefin bearing zero net charge moves toward to the metal atom of the zirconocene cation catalyst bearing a positive net charge, meaning the zirconocene undergoes a nucleophilic attack controlled by covalent interactions rather than electrostatic ones. This implies that covalent interactions predominate over electrostatic ones. When covalent interactions are more relevant than electrostatic ones, like in this case, and within the framework of Conceptual DFT,[29−35] Morell et al.[36−41] have proposed a local reactivity descriptor (LRD) which is called dual descriptor (DD) $f^{(2)}(\mathbf{r})$. In spite of having been discovered several years ago, a solid physical interpretation was not provided in the beginning.[42] Morell et al. used the notation $\Delta f(\mathbf{r})$, but currently it has been replaced by the modern notation $f^{(2)}(\mathbf{r})$ in order to highlight that this is a Fukui function of second order. Its physical meaning is to reveal, unambiguously, nucleophilic and electrophilic sites on a molecular system at the same time. Mathematically, it is defined in terms of the derivative of the Fukui function, $f(\mathbf{r})$,[32] with respect to the number of electrons,

N. Through a Maxwell relation, this LRD may be interpreted as the variation of η (the molecular hardness which measures the resistance to charge transfer[43]) with respect to $v(\mathbf{r})$, the external potential. The definition of $f^{(2)}(\mathbf{r})$ is shown as indicated by Morell et al.:[36,37]

$$f^{(2)}(\mathbf{r}) = \left(\frac{\partial f(\mathbf{r})}{\partial N}\right)_{v(\mathbf{r})} = \left[\frac{\delta \eta}{\delta v(\mathbf{r})}\right]_N \tag{1}$$

As mentioned above, DD allows one to obtain simultaneously the preferable sites for nucleophilic attacks ($f^{(2)}(\mathbf{r}) > 0$) and the preferable sites for electrophilic attacks ($f^{(2)}(\mathbf{r}) < 0$) into the system at point $\mathbf{r}$. DD has been demonstrated to be a robust tool to predict specific sites of nucleophilic and electrophilic attacks in a much more efficient way than the Fukui function by itself because dual descriptor is able to distinguish those sites of true nucleophilic and electrophilic behavior; as as consequence, some works have been published with the aim of remarking on the powerfulness of $f^{(2)}(\mathbf{r})$ and all those LRDs depending on DD.[38−40,44−46]

The general working equation to obtain DD is given by the arithmetic difference between nucleophilic and electrophilic

Table 1. Units

LRD	dimension symbol	atomic units	international system
Electron density $\rho(\mathbf{r})$	$[QL^{-3}]$	$=1$ (a.u. of charge)·(a.u. of length)$^{-3}$ $=1$ (a.u.)·bohr^{-3} $=1$ bohr^{-3}	1 C·m^{-3}
Local softness $\left(\dfrac{\partial\rho(r)}{\partial\mu}\right)_{\upsilon(r)}=s(\mathbf{r})$	$[Q^2\,L^{-5}\,T^2\,M^{-1}]$	$=1\dfrac{\text{(a.u. of charge)}\cdot\text{(a.u. of length)}^{-3}}{\text{(a.u. of energy)}\cdot\text{(a.u. of charge)}^{-1}}$ $=1\dfrac{\text{(a.u. of charge)}\cdot\text{bohr}^{-3}}{\text{hartree}\cdot\text{(a.u. of charge)}^{-1}}$ $=1\dfrac{\text{(a.u. of charge)}^2\cdot\text{bohr}^{-3}}{\text{hartree}}$ $=1\dfrac{\text{(a.u.)}^2\cdot\text{bohr}^{-3}}{\text{hartree}}$ $=1$ hartree$^{-1}\cdot$bohr^{-3}	1 C·m^{-3}·V^{-1}
Local hyper-softness $\left(\dfrac{\partial s(\mathbf{r})}{\partial\mu}\right)_{\upsilon(\mathbf{r})}=s^{(2)}(\mathbf{r})$	$[Q^3\,L^{-7}\,T^4\,M^{-2}]$	$=1\dfrac{\text{(a.u. of energy)}^{-1}\cdot\text{(a.u. of charge)}^2\cdot\text{(a.u. of length)}^{-3}}{\text{(a.u. of energy)}\cdot\text{(a.u. of charge)}^{-1}}$ $=1\dfrac{\text{hartree}^{-1}\cdot\text{(a.u. of charge)}^2\cdot\text{bohr}^{-3}}{\text{hartree}\cdot\text{(a.u. of charge)}^{-1}}$ $=1\dfrac{\text{(a.u. of charge)}^3\cdot\text{bohr}^{-3}}{\text{hartree}^2}$ $=1\dfrac{\text{(a.u.)}^3\cdot\text{bohr}^{-3}}{\text{hartree}^2}$ $=1$ hartree$^{-2}\cdot$bohr^{-3}	1 C·m^{-3}·V^{-2}

Fukui functions.[36] A well-known first level of approximation implies the use of the finite difference method where the sum of electronic densities of the system with one more electrons and one less electron is subtracted from the double of the total electronic density of the original system. Inasmuch as this level of approximation implies three quantum chemical computations (meaning the system under study with $N-1$, $N+1$, and N electrons) a second level of approximation has been used for some years where densities of frontier molecular orbitals provide a working equation that is easier to use, so that only the original system (N electrons) provides the needed information without taking into account information coming from the systems bearing $N+1$ and $N-1$ electrons:

$$f^{(2)}(\mathbf{r})\simeq\rho_{\mathrm{L}}(\mathbf{r})-\rho_{\mathrm{H}}(\mathbf{r}) \tag{2}$$

where densities of LUMO and HOMO are represented by $\rho_{\mathrm{L}}(\mathbf{r})$ and $\rho_{\mathrm{H}}(\mathbf{r})$, respectively. Molecular symmetry can influence the local reactivity, and it has been demonstrated that the Fukui function must conserve the symmetry;[47] as a consequence DD must do it too. As any degeneracy might arise in frontier molecular orbitals, within the framework of the second level of approximation, the author of the present work is aware of this phenomenon for which precautions have been considered, as demonstrated in former articles through the use of working equations adapted to the molecular symmetry.[48,49] The mathematical justification of the influence of degeneracy in local reactivity descriptors has been given by Cárdenas et al.[50]

The dual descriptor can be condensed through an appropriate integration within the kth atomic domain Ω_k:

$$\int_{\Omega_k}f^{(2)}(\mathbf{r})\,\mathrm{d}\mathbf{r}=f_k^{(2)} \tag{3}$$

When $f_k^{(2)}>0$ the process is driven by a nucleophilic attack on atom k which acts as an electrophilic species; conversely, when $f_k^{(2)}<0$ the process is driven by an electrophilic attack over atom k, and therefore, this atom k acts as a nucleophilic species. However DD is a subintensive property, thus meaning that its condensed values become insignificant as the size of the molecule increases. To overcome this intrinsic behavior of $f^{(2)}(\mathbf{r})$ another local reactivity descriptor has been defined, so that it permits us to measure local reactivities according to the molecular size;[38,41] thus meaning that it allows one to compare local reactivity among different compounds. Such a descriptor is the local hyper-softness whose mathematical definition is exhibited as follows:[38–40,51]

$$s^{(2)}(\mathbf{r})=\left(\frac{\partial^2\rho(\mathbf{r})}{\partial\mu^2}\right)_{\upsilon(\mathbf{r})}=\frac{f^{(2)}(\mathbf{r})}{\eta^2}-\frac{\gamma\cdot f(\mathbf{r})}{\eta^3} \tag{4}$$

where $\gamma=(\partial\eta/\partial N)_{\upsilon(\mathbf{r})}$, and it is called hyper-hardness, whose physical meaning and relevance is under study.[52]

The local hyper-softness is mathematically understood as the additive inverse of the variation of global softness with respect to an external potential at a fixed electronic chemical potential; through a Maxwell relation, it is also defined as the partial derivative of local softness[53–55] with respect to the chemical potential at a fixed external potential:

$$s^{(2)}(\mathbf{r})=-\left[\frac{\delta S}{\delta\upsilon(\mathbf{r})}\right]_{\mu}=\left(\frac{\partial s(\mathbf{r})}{\partial\mu}\right)_{\upsilon(\mathbf{r})}$$

Note that the number of electrons, N, is not restricted. This property enables the local hyper-softness to be used as a more appropriate descriptor to measure local reactivity when the molecular system under study is going to face the arrival or departure of electrons, but without defining previously a number of electrons owing to nucleophilic or electrophilic attacks, respectively. As a consequence for open-shell systems, this local reactivity descriptor permits us to quantify local reactivities consistent with the system's size.

Up to now with the rise of several descriptors, some confusion might be experienced by novel readers in the field of Conceptual DFT, hence a physical meaning of this descriptor must be provided before exposing its use. The grand canonical ensemble states that the chemical potential, μ, and the external potential, $v(\mathbf{r})$, are the fundamental variables for any system. This scheme is also known as the open-system representation because the number of electrons in a molecule fluctuates in the presence of other molecule, meaning that there is no control over the number of electrons, so that the grand potential arises as the state function that is able to represent the stability of molecules under these conditions.

Since this is a descriptor of third order, when there is any doubt about information provided by local softness, the local hyper-softness allows one to unambiguously distinguish the actual nucleophilic or electrophilic nature of a region on a molecule in agreement with the molecular size, so that the use of this descriptor to establish comparisons among molecules of different sizes is possible to perform; on the contrary, the dual descriptor cannot be used for these intermolecular comparisons, since it only gives information about the local reactivity at an intramolecular level.

First of all, a dimensional analysis must be carried out. After defining M, L, T, and Q as general symbols for mass, length, time, and electric charge, respectively, the very first three local reactivity descriptors within the open-system representation are expressed in atomic units along with the units belonging to the international system of units as indicated by Table 1.

For those who are not familiarized with the Conceptual DFT, a definition for each of these units will be given. For instance, it is said that the electron density, $\rho(\mathbf{r})$, is equal to 1 a.u. (or 1 bohr^{-3}) when one electron is found in a volume of 1 cubic bohr (1 bohr·1 bohr·1 bohr). As a consequence, the local softness, $s(\mathbf{r})$, is equal to 1 a.u. (or 1 hartree^{-1}·bohr^{-3}) when the electron density varies in 1 bohr^{-3} because of an experienced change by the chemical potential, μ, in 1 hartree. It is worthwhile to mention that the chemical potential is equal to 1 a.u. (or 1 hartree) when one electron has the trend of 1 hartree in energy to escape from the equilibrium system. With these definitions the physical meaning of the local hyper-softness can be deduced as follows: it is said that the local hyper-softness, $s^{(2)}(\mathbf{r})$, is 1 a.u. (or 1 hartree^{-2}·bohr^{-3}) when the local softness varies in 1 hartree^{-1}·bohr^{-3} because of a change experienced by the chemical potential in 1 hartree.

It is easy to deduce that from eq 4, the terms $f^{(2)}(\mathbf{r})/\eta^2$ and $(f(\mathbf{r})/\eta^3)\gamma$ have the same units: hartree^{-2}·bohr^{-3}. Since the bohr is an atomic unit of length, the hartree unit can be transformed into eV avoiding an explicit writing of the length unit according to

$$1 \text{ hartree}^{-2}\cdot\text{bohr}^{-3} \equiv 1 \text{ hartree}^{-2} = 1.35051\cdot10^{-3} \text{ (eV)}^{-2}$$
$$= 1.35051 \text{ m(eV)}^{-2}$$

Since γ is negligible,[38] the respective working equation is expressed as follows:

$$s^{(2)}(\mathbf{r}) \simeq f^{(2)}(\mathbf{r})\cdot S^2 \tag{5}$$

where S stands for the global softness,[31,32,43] which can be calculated in terms of HOMO and LUMO energies provided that Koopmans' theorem[56] is satisfied as several articles have demonstrated:[31,32,43]

$$S \simeq (\varepsilon_L - \varepsilon_H)^{-1} \tag{6}$$

where ε_L and ε_H stand for the LUMO and HOMO energies, respectively. Nevertheless, some doubts about the use of this theorem have been exposed by Joubert,[57] since the LUMO computed in a traditional Kohn–Sham DFT calculation corresponds to electronic excitation, not electron attachment.[58,59] Even so, the information coming from Koopmans' theorem would provide a valid qualitative picture about molecular reactivity. Besides, some authors have claimed that γ has a chemical meaning,[52] so a working equation including this term should be proposed. At the moment, the use of eq 5 is sufficient for the purpose of this work where $s^{(2)}(\mathbf{r})$ is computed by the use of eqs 6 and 2.

Similarly, the local hyper-softness can also be condensed through an appropriate integration within the kth atomic domain Ω_k:

$$\int_{\Omega_k} s^{(2)}(\mathbf{r}) \, d\mathbf{r} = s_k^{(2)}$$

Then, the use of local hyper-softness allows one to ensure that the measurement of local reactivity on a molecular system can be comparable with local reactivity of other systems without considering differences in size. This descriptor should be able to measure electronic inductive effects in agreement with the molecular size. The obtention of integrated values of $s^{(2)}(\mathbf{r})$ are explained in Computational Methods. When the catalytic activity is mainly controlled by electronic inductive effects and not by steric effects, the hypothesis is that a higher condensed value of $s_{Zr}^{(2)}$ leads to a higher value of catalytic activity, and when the steric effect seems to provide a contradictory explanation, the local hyper-softness allows one to understand that catalytic activity is driven mainly by electronic inductive effects.

3. COMPUTATIONAL METHODS

All metallocene cations were geometrically optimized; frequency calculations were then performed to identify the stationary points as minima.[60] The functionals used in the present calculations are the Becke-3 for exchange and Lee–Yang–Parr for correlation (B3LYP).[61−64] The basis set used for nonmetal atoms is 6-31G(d)[65,66] and LANL2DZ[67−69] with effective core potentials for Zr. All calculations were carried out using the Gaussian 09[70] software package. For obtaining integrated values of Fukui function, the Fukui Rev 1.1 software was used[71−74] where nucleophilic and electrophilic Fukui functions are condensed according to references just mentioned for this software, meaning all of the condensed values of dual descriptor are computed as a simple arithmetic difference between f_k^+ and f_k^-, respectively, in order to obtain $f_k^{(2)}$. Condensed values of $s^{(2)}(\mathbf{r})$ are obtained as an ordinary multiplication between S^2 and $f_k^{(2)}$. All of the zirconocene methyl cations have been organized into two types of subgroups depicted by Figures 2 and 3: A, B, and C whose

experimental data were obtained at 60 °C and subgroups D, E, and F where the experimental information was obtained at a 10 °C.

4. RESULTS AND DISCUSSION

If the electronic inductive effect predominates over the steric effect, then a linear-like trend is expected between the condensed value of the local hyper-softness on the metal and the logarithm of catalytic activity. The reason for defining subgroups lies in the fact that a possible marked influence of steric effect must be minimized in order to establish comparisons among different zirconocene cationic catalysts. A way to carry out this procedure is by comparing those catalytic systems presenting relevant structural resemblances. This would provide a rational explanation for differences mainly in terms of electronic inductive effects, although the steric influence cannot be completely ignored; therefore, cases where the steric effect predominates over the electronic inductive effect in spite of this classification are not rare. These cases will be detected as noticeable deviations in graphics of the following type: local hyper-softness condensed on the metal against the logarithm of catalytic activity.

As a graphical example of local hyper-softness, Figure 4 clearly represents a nucleophilic attack performed by an
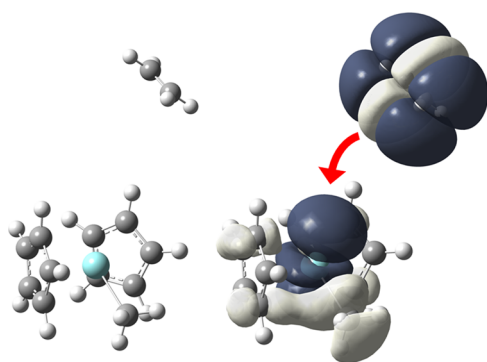

Figure 4. Left figure corresponds to a ball-and-stick model for MZ001 and an ethylene molecule above it; right figure is a 3D map of local hyper-softness surrounding MZ001 and the same descriptor surrounding the ethylene molecule. A dark-colored lobe implies that $s^{(2)}(\mathbf{r}) > 0$, thus indicating that nucleophilic attacks will preferentially occur there; a light-colored lobe implies that $s^{(2)}(\mathbf{r}) < 0$, thus indicating that electrophilic attacks will preferentially occur there. A favorable interaction between two species is ruled by a maximum overlap between $s^{(2)}(\mathbf{r}) < 0$ of ethylene and $s^{(2)}(\mathbf{r}) > 0$ of the metallocene cation. As observed, there is a flow of π-electrons coming from ethylene toward the metal atom as indicated by the red arrow that justifies the coordination of ethylene onto the metallocene cation. Isosurface is depicted at 0.0001 a.u.

ethylene molecule, since π-electrons of ethylene are easier to remove and as a consequence are attracted to the metal center of the metallocene cation. Besides, the reader can run a single point calculation at the same level of theory in order to check that the chemical potential of ethylene (-3.37 eV) is higher than the chemical potential of the respective zirconocene methyl cation (Tables 2 and 3), hence there is no doubt that the electron flow departs from the ethylene and not from the zirconocene methyl cation. According to local hyper-softness, there is a favorable match between π-electrons of ethylene (light-colored lobe around ethylene) and the zirconium atom of zirconocene methyl cation (dark-colored lobe around the

Table 2. [a]

	metallocenic cation	μ	Log{CatAct}	$s_{Zr}^{(2)}$
Subgroup A	MZ001	−8.99	3.17	52.27
	MZ002	−8.02	**3.51**	**74.31**
	MZ003	−7.90	3.00	69.21
	MZ004	−7.56	2.85	61.06
	MZ005	−7.43	2.63	76.81
Subgroup B	MZ021	−7.59	3.39	56.14
	MZ022	−7.28	3.47	63.35
	MZ023	−8.20	3.54	55.10
	MZ024	−8.06	3.58	57.83
	MZ025	−7.80	**4.18**	**87.76**
Subgroup C	MZ001	−8.99	3.17	52.27
	MZ026	−8.14	**3.76**	**56.45**
	MZ027	−7.79	1.88	42.97
	MZ028	−7.31	2.36	49.90
	MZ029	−7.45	2.65	49.80

[a] Chemical electronic potential, μ, is expressed in eV; base-10 logarithm of catalytic activity[28] (Log{CatAct}), where CatAct is expressed in kilograms of polyethylene per gram of metallocene per hour and local hyper-softness, $s_{Zr}^{(2)}$, that is expressed in m(eV)$^{-2}$ and condensed on the Zr atom. According to the literature, catalytic activities were obtained at 60 °C.

Table 3. [a]

	metallocenic cation	μ	Log{CatAct}	$s_{Zr}^{(2)}$
Subgroup D	MZ003	−7.90	2.24	69.21
	MZ031	−7.79	2.18	66.81
	MZ032	−7.81	**2.48**	**75.59**
	MZ033	−7.80	2.20	68.34
	MZ034	−7.75	2.40	80.99
Subgroup E	MZ003	−7.90	2.24	69.21
	MZ035	−7.55	2.34	62.96
	MZ036	−7.46	1.64	62.97
	MZ038	−7.61	2.24	63.22
Subgroup F	MZ003	−7.90	2.24	69.21
	MZ039	−7.39	**2.61**	**78.40**
	MZ040	−7.13	2.24	51.12
	MZ041	−7.19	1.94	52.29
	MZ042	−7.35	2.44	82.99

[a] Chemical electronic potential, μ, is expressed in eV; base-10 logarithm of catalytic activity[28] (Log{CatAct}), where CatAct is expressed in kilograms of polyethylene per gram of metallocene per hour and local hyper-softness, $s_{Zr}(2)$, that is expressed in m(eV)$^{-2}$ and condensed on the Zr atom. According to the literature, catalytic activities were obtained at 10 °C.

metal), thus resulting in the coordination of ethylene on the metallocene cation (Figure 4).

The chemical intuition indicates that the influence of steric effect can be easily inferred in the sense that a decrease of the catalytic activity is expected as a result of an increase of substituent groups' size, especially if the reactivity site under analysis is being blocked by bulky substituent groups, but this deduction can only be described after watching the molecular model of the structure under analysis. The quantification of a steric effect is still a matter of debate,[75−80] and there is no a unique procedure to carry out such an estimation. Even so, it is still possible to detect a predominance of steric or electronic effects;[81] in fact, some new calculations are being carried out in order to quantify locally the steric effect with the aim of establishing a type of correlation among catalytic activity and
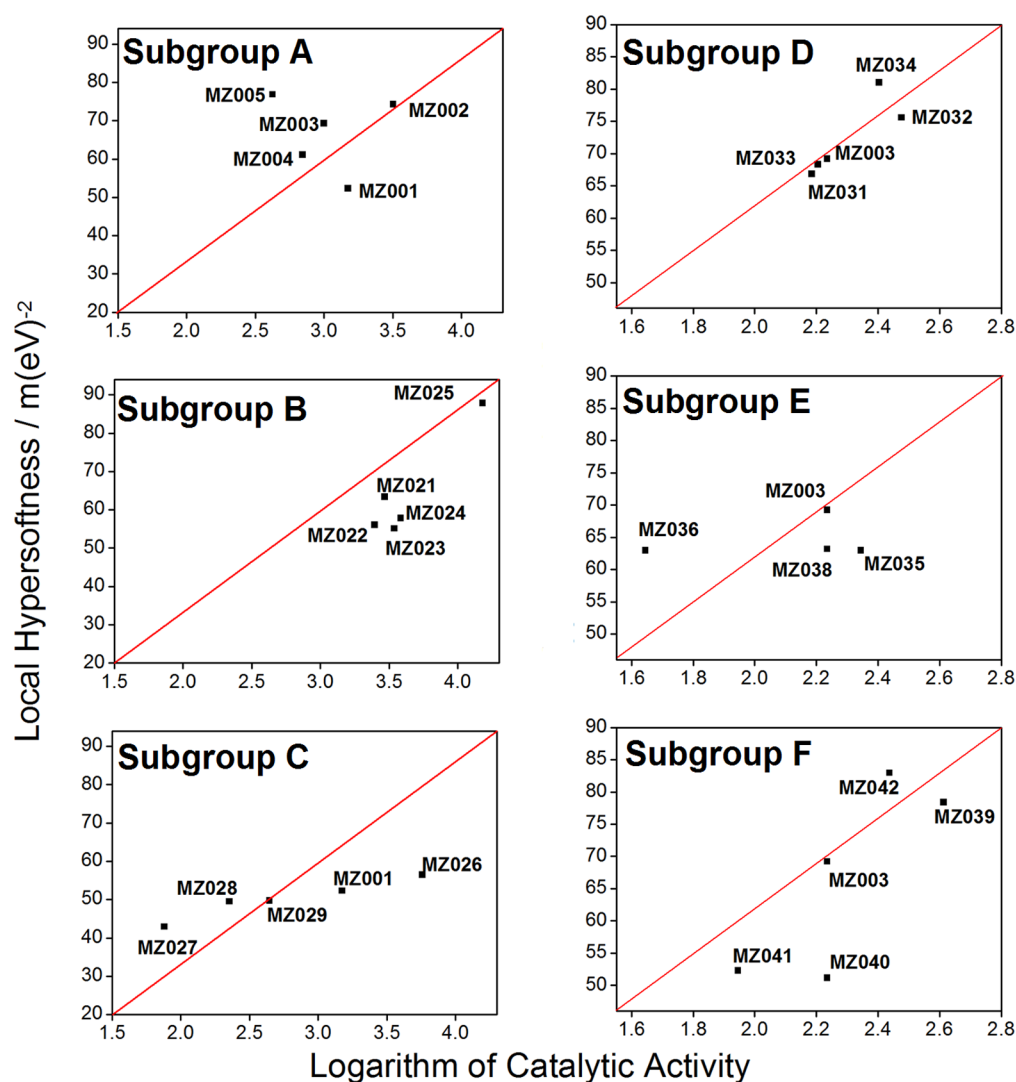
Figure 5. Graphical plots of local hyper-softness versus base-10 logarithm of catalytic activity for A, B, C, D, E, and F subgroups. Laboratory conditions: catalytic activities (CatAct) are expressed in kilograms of polyethylene per gram of metallocene per hour and per pressure unit, the solvent is *n*-pentane, and the ethylene pressure is 10.0 bar. All experimental values reported in such review were obtained at 60 °C for subgroups A, B, and C and 10 °C for subgroups D, E, and F.

both electronic inductive and steric effects. However, for the purpose of this article, such a tool has not been used because this work is focused on explaining some cases where the chemical intuition associated to an apparent steric effect fails when trying to understand differences that are detected between a couple of catalysts that differ only slightly or not at all in their molecular structures. In these cases where the steric effects cannot be used as a sufficient argument to explain differences in catalytic activity, only the use of a descriptor able to quantify electronic effects is required, and local hyper-softness has been demonstrated to be suitable enough for such purposes. As a graphic example, the nucleophilic attack of π-electrons coming from ethylene toward the zirconium atom of MZ001 can be depicted as a 3D map of the local hyper-softness (Figure 4).

The dark-colored lobe of this descriptor implies $s^{(2)}(\mathbf{r}) > 0$, meaning that nucleophilic attacks will be oriented there; a light-colored lobe implies that $s^{(2)}(\mathbf{r}) < 0$, meaning that electrophilic attacks will be headed there. Since the interaction between an ethylene molecule and a zirconocene methyl cation implies a nucleophilic attack from π-electrons of ethylene toward the

zirconium atom of the metallocene methyl cation to give rise the Cossée−Arlman's π-complex, this π-complex experiences a noticeable intramolecular rearrangement in such a way that the methyl group migrates toward to the coordinated ethylene thus leading to a propyl chain that sets free the coordination site again, so allowing the coordination of a second ethylene molecule and so on. This is the process that explains the increase of the carbon chain length along the entire polymerization process. Local hyper-softness was condensed on the metal center on each zirconocene methyl cation and the obtained values are quoted in Tables 2 and 3; catalytic activity data were extracted from the respective bibliography;[28] all of the metallocene cationic systems were classified in subgroups in order to simplify the comparison among those catalysts that are structurally similar each other as explained in the Computational Methods section.

From Tables 2 and 3 it is inferred that some kind of order relationship exists that allows one to claim that when steric effects are not predominant, the electronic inductive effects control the catalytic activity, which is well quantified by means of the local hyper-softness:

i. Log{CatAct} a pure experimental parameter)

Subgroup A: MZ002 > MZ001 > MZ003 > MZ004
> MZ005

Subgroup B: MZ025 > MZ024 > MZ023 > MZ021
> MZ022

Subgroup C: MZ026 > MZ001 > MZ029 > MZ028
> MZ027

Subgroup D: MZ032 > MZ034 > MZ003 > MZ033
> MZ031

Subgroup E: MZ035 > MZ038 = MZ003 > MZ036

Subgroup F: MZ039 > MZ042 > MZ003 = MZ040
> MZ041

ii. $s_{Zr}^{(2)}$ (a pure theoretical parameter)

Subgroup A: MZ005 > MZ002 > MZ003 > MZ001
> MZ004

Subgroup B: MZ025 > MZ021 > MZ024 > MZ022
> MZ023

Subgroup C: MZ026 > MZ001 > MZ029 ≈ MZ028
> MZ027

Subgroup D: MZ034 > MZ032 > MZ003 > MZ033
> MZ031

Subgroup E: MZ003 > MZ038 ≈ MZ035 > MZ036

Subgroup F: MZ042 > MZ039 > MZ003 > MZ041
> MZ040

Figure 5 provides partial information to acquire some understanding about the catalytic activity values in terms of electronic inductive effects that are quantified through the use of local hyper-softness that is condensed on the metal. The red line only helps the reader to identify a possible linear trend. If so, this means that the influence of steric effect is overcome by the influence of electronic inductive effect. Noticeable deviations from this linearity reveal a predominance of steric effect over electronic inductive effect. The analysis was split into six subgroups as follows.

4.1. Subgroup A. According to Figure 2, clearly both MZ001 and MZ002 differ in their ligands, so chemical intuition would indicate that MZ001 might have higher catalytic activity in comparison with MZ002, but experimental evidence reveals the contrary (Figure 1 and graphic entitled Subgroup A of Figure 5); in fact, MZ002 has high catalytic activity that is pretty noticeable when compared with the remaining metallocene cations of this subgroup. Clearly the steric effect cannot be used as a conceptual support to explain this apparent anomaly. In this case, the electronic inductive effect helps explain it because, from Table 2, it is inferred that local hyper-softness centered on the metal of MZ002 shows a value larger than the condensed one on the metal of MZ001. As a result, the steric effect is much less important here than the electronic inductive effect. On the other hand, MZ003, MZ004, and MZ005 deviate markedly from linearity, and then it is suspected that for these last metallocene cations the steric effect predominates over the electronic inductive effect because, as can be noted, MZ005 possesses the highest value for the condensed local hyper-softness on the metal. However, this catalyst presents the lowest value of catalytic activity and, as a consequence, the condensed value of the local hyper-softness cannot be directly associated to the catalytic activity; the same conclusion is reached for MZ004 and MZ003. The only reason to explain this apparent contradiction is given by its bulky ligands (two fluorenyl groups in the case of MZ005) that helps to partially block the coordination site, that is to say, the metal atom. Hence, it does not matter if the metal atom presents the highest reactivity to coordinate an ethylene molecule because the access to this site is partially blocked by bulky ligands. A similar explanation can be used for MZ004 and MZ003 which possess bulky ligands, but in the case of MZ004, just one ligand corresponds to fluorenyl and the another ligand is indenyl: then, it makes sense that its catalytic activity is slightly higher than that of MZ005. The catalytic activity of MZ003 is slightly higher than that of MZ004; this is because MZ003 has only one fluorenyl group while the second ligand is cyclopentadienyl. What we have learned so far is that, while the influence of the steric effect on values of catalytic activity can be inferred by watching the molecular structure of catalysts to understand differences that are observed in this pure experimental parameter, although the influence of the electronic inductive effect cannot possibly be inferred in the same way, the condensed local hyper-softness has been demonstrated to be an appropriate index to acquire a sensible understanding of such differences in catalytic activities. Then, when electronic inductive effects are suspected to be responsible for observed differences in catalytic activities and not the steric effects, this local reactivity descriptor should be used.

4.2. Subgroup B. This set of catalysts (Figure 2) is interesting to study too, because it presents two kinds of ligands: indenyl and cyclopentadienyl. From Table 2 respective catalytic activities and condensed local hyper-softness values are quoted in order to give rise to the graphic entitled Subgroup B of Figure 5. The only difference in these catalytic systems is given by the presence of some substituent groups located at positions 1 and/or 2 or 3 in indenyl ligand. It is possible to realize that MZ022 has two bulky substituents in its indenyl ligand, and although the condensed value of its local hyper-softness on the metal is not the lowest one, but rather one of the lowest, it is not surprising that the catalytic activity is the lowest in this subgroup. MZ021 and MZ023 have one substituent group at the position 2 of indenyl. The respective condensed values of local hyper-softness on metal reveal that MZ021 is more reactive than MZ023: then, if the electronic inductive effect predominates over the steric one, the experimental result would indicate higher catalytic activity for MZ021 than that of MZ023. However, experimentally, the contrary occurs. The only explanation is based on steric effects: since the phenyl group in MZ021 is bulkier than the methyl group in MZ023, this experimental evidence indicates that the catalytic activity in MZ023 is slightly higher than that of MZ021. Then, differences in catalytic activity between MZ023 and MZ021 are explained in terms of steric effects because they predominate over the electronic inductive effects. So far, the differences of catalytic activity among MZ021, MZ022, and

MZ023 can be explained in terms of steric effects and the use of the local hyper-softness was unnecessary. It seems the analysis becomes more difficult for the remainder. For instance, MZ024 has two methyl groups at 1 and 2 positions of indenyl, while MZ023 has only one methyl group at the 2 position of its ligand indenyl. Then, it would be sensible for lower catalytic activity for MZ024 to be expected in comparison with MZ023. The experimental evidence reveals the contrary situation again. This apparent contradiction from the steric point of view must be solved in terms of electronic inductive effects. After using the local hyper-softness, it turns out that the condensed value of this descriptor on the metallic atom of MZ024 is higher than that on the metallic atom of MZ023, meaning that ethylene coordination on the metallic atom of MZ024 is more favorable than that of the metallic atom of MZ023; this makes sense since the same order relationship is found in catalytic activity of MZ024 and MZ023. The catalyst MZ025 has one substituent group at 1 position of indenyl. This substituent group is phenyl and, similarly to MZ022, one would expect an unfavorable role for the catalytic activity. That would be true when the steric effect predominates over the electronic inductive effect, and as a consequence, MZ025 would have a similar value of catalytic activity as was exhibited by MZ022. However, MZ025 has the highest catalytic activity in Subgroup B. Immediately, one can suspect that electronic inductive effects are driving the catalytic activity and not the steric effects. To answer this question, the local hyper-softness condensed on the metallic atom of MZ025 should result into a high value. As expected, the condensed value of this local reactivity descriptor on the metallic atom is the highest in Subgroup B. Definitely, MZ025 has the highest value of catalytic activity in this subgroup only by electronic inductive reasons and not by steric reasons.

4.3. Subgroup C. Values of catalytic activities and condensed local hyper-softness of catalysts (Figures 2 and 3) depicted in Figure 5 were calculated and exhibited in Table 2. Three of these catalysts (MZ027, MZ028, and MZ029) possess one very large ligand corresponding to tris(pyrazolyl)borate; therefore, it is expected that they present the lowest catalytic activities in comparison with MZ001 and MZ026. So, it is possible to state that the differences in these values of catalytic activity are given by steric reasons. Now, when observing in more detail the MZ027, MZ028, and MZ029 systems, differences among them are not given by steric reasons. It is a surprise to find that MZ027 has lower catalytic activity than MZ028 and MZ029. MZ027 has a cyclopentadienyl ligand, while both MZ028 and MZ029 systems have an indenyl ligand, which occupies a bigger volume in space in comparison with cyclopentadienyl. This seems to be an apparent contradiction. However, when comparing with differences that are found between MZ001 and MZ002 in Subgroup A, one can deduce that an indenyl ligand exerts an important electronic inductive effect that favors ethylene coordination on the metallic atom. Such electronic inductive effect is not exerted with the same intensity by cyclopentadienyl. To check this statement, let us see the causes for the observed differences in catalytic activity between MZ001 and MZ026. Again, a catalytic system with a bulkier ligand (MZ026) is compared with a catalytic system with two cyclopentadienyl ligands (MZ001) which are less bulky. The bulky ligand in MZ026 corresponds to an indenyl with a methyl group at the 1 position. Then, it is possible to claim that MZ026 has higher catalytic activity than MZ001 because of reasons based on electronic inductive effects; this is supported by the values of local hyper-softness: the condensed

value of this local descriptor on zirconium of MZ026 is larger than the same descriptor that is condensed on zirconium of MZ001. The reader can appreciate this statement better by the graphic entitled Subgroup C in Figure 5; it is interesting to notice that all of these catalytic systems seem to follow a linear trend, so that those systems bearing bulky substituents appear in the lower left position of this graphic and the remainder (MZ001 and MZ026) appear slightly in the upper right position of the same graphic.

To sum up, differences that are found in values of catalytic activities between {MZ027,MZ028,MZ029} and {MZ001,MZ026} are mainly supported by steric reasons, but among MZ027, MZ028, and MZ029, the differences found in catalytic activity are explained in terms of electronic inductive effects exerted by the indenyl ligand, which favors a coordination of ethylene on metallic atom because values of condensed local hyper-softness on the metallic atom are favoring MZ028 and MZ029, but not MZ027; therefore, these two systems (MZ028 and MZ029) have higher catalytic activity than that of MZ027.

Subgroups A, B, and C were analyzed separately and all together, because all of their experimental parameters were collected exactly at the same experimental conditions. The following analysis concerning subgroups D, E, and F implies another temperature,[28] so a direct comparison with A, B, and C is not possible.

4.4. Subgroup D. These catalytic systems are made of cyclopentadienyl (Cp) and fluorenyl (Flu) ligands bearing just one methyl group as a substituent in the Flu ligand. These systems (MZ003, MZ031, MZ032, MZ033, and MZ034) are distinguishable by different positions of methyl group either on the six-membered ring or on the five-membered ring of Flu, as observed in Figure 3. In this case, all of the catalysts are quite similar and immediate evidence is given by a linear trend observed in the graphic entitled Subgroup D of Figure 5. In the paper written by Alt and Köppl,[28] MZ003 and MZ030 have exactly the same molecular structure, but their experimental parameters were collected at different temperatures, thus reporting a couple of different values of catalytic activity which are not comparable between them; however, the local reactivity descriptors used here are not temperature-dependent, and for that reason only one value for this descriptor exists. As a consequence, only with the aim of showing the molecular structure, the MZ003 notation was used instead of MZ030. The relationship was established with the catalytic activity obtained under the experimental conditions belonging to MZ030, as it should be; all of this in order to maintain the consistency when comparing with the remaining members of this subgroup. The observed linear trend reveals that the steric effect is almost negligible and constant, so that the influence of the electronic inductive effect predominates throughout this subgroup, and as a consequence it is possible to claim that this subgroup is also suitable to assess capabilities of any other descriptor that has been proposed to measure the electronic inductive effect. However, it is important to remark that MZ034 escapes from this qualitative tendency because, in spite of exhibiting the highest condensed value of local hyper-softness on Zr, this catalyst is not the one that exhibits the highest catalytic activity value. In such a case, the steric effect can be used again as a valid argument to justify this deviation. One reason is that MZ034 is the only catalyst in this subgroup whose methyl group is localized at 9 position, which is closer to the metallic atom in comparison with the remaining positions on Flu, thus

helping to block the coordination site (Zr atom). This explains the inconsistency between the catalytic activity and the condensed value of the local hyper-softness on the metal in MZ034.

4.5. Subgroup E. Except for MZ003, this subgroup is characterized because the MZ035, MZ036, and MZ038 cations have substituent groups at positions 2 and 7 of Flu. There is no appreciable linear trend, but it is interesting to remark some characteristics that are deduced from the graphic entitled Subgroup E of Figure 5. For instance, although MZ003 shows the highest condensed value of local hyper-softness, it does not present the highest value of catalytic activity. Rather than MZ003, the MZ035 presents the highest catalytic activity, in spite of having a lower condensed value of local hyper-softness than MZ003 and bulky substituents at 2 and 7 positions of Flu. Bearing in mind that the catalytic activity should be a resultant experimental parameter as a consequence of steric and electronic inductive effects, if the local hyper-softness does not favor the reactivity of Zr in MZ035, then the steric effect should be responsible for MZ035 showing a higher catalytic activity than MZ003. This would be an example where the steric hindrance favors rather than prevents the coordination of an olefin molecule. Although not computed in this work, it seems that according to the considerable size of Flu, a free internal rotation of it with respect to the Zr atom would imply a difficult coordination of olefin, while if this internal rotation is impeded by some bulky substituents at the 2 and 7 positions of Flu, the coordination of an olefin might be favored. According to this qualitative assumption, and returning to the analysis on this subgroup, although *tert*-butyl is a bulky substituent located at 2 and 7 positions of Flu, and the local reactivity of the respective cation is lower than that of MZ003, it is suggested that owing to the steric hindrance of *tert*-butylfluorenyl, the resulting catalytic activity of MZ035 is the highest in this subgroup. This statement should be checked by means of an analysis of the internal rotation of *tert*-butyl in comparison with the internal rotation experienced by the fluorenyl ligand without substituent groups: this is a pendant task that will help understand the suggested explanation and will be an issue of another article because measurement of the steric effect is not an aim in this work. On the other hand, it is possible to note that MZ003 and MZ038 exhibit almost the same value of catalytic activity, but MZ003 has a value of condensed local hyper-softness on the metal that is higher than that of MZ038. Due to steric hindrance, intuitively one would expect that MZ038 would have a smaller catalytic activity than that of MZ003. However, as MZ038 has 1-methylvinyl substituent groups at 2 and 7 positions of Flu, if using the same qualitative argument as used for MZ035, then the steric effect turns out to be favorable for an olefin coordination; as a result, the catalytic activity of MZ038 is not smaller than that of MZ003, but rather it is almost the same as that observed in Figure 5. Finally, MZ036 is not very different when comparing its condensed value of local hyper-softness with those ones of MZ035 and MZ038. However, MZ036 has the lowest catalytic activity in this subgroup, meaning that the steric effect is not playing a favorable role, but rather unfavorable. One reason could be based on the fact that MZ036 possesses methoxy groups at 2 and 7 positions, which can experience internal rotation around the oxygen—carbon bond that seems to be easier than the internal rotation that *tert*-butyl and 1-methylvinyl groups might experience. This discussion indicates that finding a definitive set of reasons allowing one to understand and explain catalytic

activities only in terms of steric and electronic inductive effects is still a difficult task to do. In the presence of complex substituent groups that could experience some internal rotation, the final effect would be either an increase or decrease of the catalytic activity, but there would be no certainty in knowing such an effect previously without computing the internal rotations.

4.6. Subgroup F. This subgroup is characterized because there is one substituent group located at the 9 position of Flu. As can be observed in Figure 3, both MZ039 and MZ042 systems have a *tert*-butyl and a cyclohexyl, respectively. On the other hand, MZ040 has a phenyl and MZ041 bears a 4-fluorophenyl; the MZ003 system does not have a substituent group. Then, according to the values of local hyper-softness condensed on the metal, it is possible to realize that an aromatic substituent group at the 9 position of fluorenyl tends to lower the condensed value of the local hyper-softness on the zirconium; on the contrary, an alkyl substituent group increases the condensed value of the local hyper-softness on the zirconium. The steric effect would explain subtle differences that are found between condensed values of local hyper-softness of MZ039 and that of MZ042: MZ039 has a *tert*-butyl substituent group which is less bulky than the cyclohexyl substituent group and, as a result, the catalytic activity of MZ039 is higher than that of MZ042 as observed in Figure 5. Similarly, this steric reason is used to understand the differences found in condensed values of local hyper-softness on zirconium between MZ040 and MZ041: The 4-fluorophenyl substituent group of MZ041 is slightly bulkier than the phenyl substituent group of MZ040, thus allowing us to understand that the catalytic activity of MZ040 is higher than that of MZ041.

As a general comment concerning all of these subgroups (A, B, C, D, E, and F), it is noticeable that the highest value of catalytic activity on each subgroup is associated with one the highest values of condensed local hyper-softness on the zirconium; these values have been highlighted in bold-face style as exposed by Tables 2 and 3. A clear exception is observed in subgroup E where this kind of rule is not satisfied at all due to the complex structure of substituent groups as explained before.

5. CONCLUSIONS

In the field of catalysis and in reference to the electronic inductive effect, the main advantage of using the local hyper-softness descriptor, which is condensed on a strategic site of the catalytic system, lies in the fact that this is a reactivity descriptor that is consistent in size, thus allowing one to establish comparisons of local reactivity among catalytic systems of different sizes; this is not possible to carry out with the dual descriptor by itself. On the other hand, although the measure of steric effects is still an issue of debate, a qualitative idea of this concept is acquired by a simple inspection of the molecular structure. So, according to the bulky nature of substituent groups and their orientation in space, it would be possible to infer whether the catalytic activity is going to be favored or not by the steric effect. When values of catalytic activity cannot be explained in terms of a qualitative appreciation of the substituent groups' volume, the electronic inductive effect is a proper argument which can be measured by the local hyper-softness descriptor. In this way, it is possible to understand if an experimental key parameter such as the catalytic activity is being controlled by steric effects or electronic inductive effects.

Nevertheless, an issue that was not broached in detail in this work has to do with the optimized geometrical structure of metallocene cations that were analyzed in the present work. These cations might have more than one conformation of minimum energy on the potential energy hyper-surface, so that small changes in their geometrical conformation might enhance or diminish the studied electronic inductive and steric effects. In the present case, these effects were assessed in just one conformation of minimum energy without taking into account all of the possible conformations of minimum energy. Even more, the exploration of reactivity on molecular geometries that have been optimized as transition states has not been done yet, so this kind of analysis might be more useful than using conformations that have been found on positions located at minima of the potential energy hyper-surface, because a zirconocene methyl cation that has been optimized as a transition state is the best conformation that could be required to coordinate an olefin. This was not taken into account in the present work.

So far, the catalytic activity has been interpreted in terms of condensed values of the local hyper-softness to measure the electronic inductive effect and in terms of a qualitative appreciation of steric effects. However, to predict or estimate catalytic activity values, both steric and electronic inductive effects must be taken into account quantitatively and accurately. None of these effects must be considered in an independent way; however, for the purposes of this article, the precaution in selecting some subgroups of metallocene cations has been considered to assess the quality of the local hyper-softness and to use it as a suitable local reactivity descriptor of the electronic inductive effect, because sometimes values of electronic inductive effects predominate over the steric effects, but this does not mean that the steric effect is not operating on the reactivity of the catalytic system.

This work has been motivated because it is usually thought that the majority of catalytic activity values are controlled, in the first place, by steric effects and, in the second place, by electronic inductive effects which play a role that sometimes can overcome the importance played by steric effects. The local hyper-softness along with another descriptor that should be able to quantify the steric effect properly should lead to a possible estimation or prediction of catalytic activity. To sum up, the local hyper-softness can be considered as a complementary tool when the steric effect is not a sufficient reason to explain some values of catalytic activity. A study to estimate catalytic activity by taking into account the steric effect along with the electronic inductive effect is in progress and it is expected to be published in the long term.

■ AUTHOR INFORMATION

Corresponding Author
*E-mail: jmartiar@gmail.com; jmartiar@uc.cl.

Notes
The authors declare no competing financial interest.

■ REFERENCES

(1) Kaminsky, W.; Külper, K.; Brintzinger, H. H.; Wild, F. R. W. P. Polymerization of Propene and Butene with a Chiral Zirconocene and Methylalumoxane as Cocatalyst. *Angew. Chem., Int. Ed. Engl.* **1985**, *24*, 507−508.

(2) Schuntenhaus, H.; Brintzinger, H. H. 1,1′-Trimethylenebis(η^5 5-3-*tert*-butylcyclopentadienyl)-titanium(iv)dichloride, a Chiral Ansa-titanocene Derivative. *Angew. Chem., Int. Ed. Engl.* **1979**, *18*, 777−778.

(3) Wild, F. R. W. P.; Zsolnai, L.; Huttner, G.; Brintzinger, H. H. Ansa-metallocene Derivatives: IV. Synthesis and Molecular Structures of Chiral Ansa-titanocene Derivatives with Bridged Tetrahydroindenyl Ligands. *J. Organomet. Chem.* **1982**, *232*, 233−247.

(4) Heiland, K.; Kaminsky, W. Comparison of Zirconocene and Hafnocene Catalysts for the Polymerization of Ethylene and 1-Butene. *Makromol. Chem.* **1992**, *193*, 601−610.

(5) D'Agnillo, l.; Soares, J. B. P.; Penlidis, A. Effect of Operating Conditions on the Molecular Weight Distribution of Polyethylene Synthesized by Soluble Metallocene/Methylaluminoxane Catalysts. *Macromol. Chem. Phys.* **1998**, *199*, 955−962.

(6) Kaminsky, W. New Polymers by Metallocene Catalysis. *Macromol. Chem. Phys.* **1996**, *197*, 3907−3945.

(7) Frauenrath, H. *Polymerization of Olefins and Functionalized Monomers with Zirconocene Catalysts*, PhD thesis, Fakultät für Mathematik, Informatik und Naturwissenschaften der Rheinisch-Westfälischen Technischen Hochschule Aachen, October 2001.

(8) Cruz, V. L.; Muñoz-Escalona, A.; Martínez-Salazar, J. A Theoretical Study of the Comonomer Effect in the Ethylene Polymerization with Zirconocene Catalytic Systems. *J. Polym. Sci., Part A: Polym. Chem.* **1998**, *36*, 1157−1167.

(9) Petitjean, L.; Pattou, D.; Ruiz-López, M. F. Theoretical Study of Selectivity Mechanisms in Propylene Polymerization with Metallocene Catalysts. *J. Mol. Struct. (Theochem)* **2001**, *541*, 227−235.

(10) Corradini, P.; Cavallo, L.; Guerra, G. Molecular Modeling Studies on Stereospecificity and Regiospecificity of Propene Polymerization by Metallocenes. In *Metallocene-Based Polyolefins*; Scheirs, J., Kaminsky, W., Eds.; John Wiley & Sons Ltd.: Chichester, 2000; Vol. 2, pp 3−36.

(11) Woo, T. K.; Deng, L.; Margl, P. M.; Ziegler, T. Computational Modeling of Single-Site Olefin Polymerization Catalysts. In *Metallocene-Based Polyolefins*; Scheirs, J., Kaminsky, W., Eds.; John Wiley & Sons Ltd.: Chichester, 2000; Vol. 2, pp 69−88.

(12) Martínez Araya, J. I. *Estudio Teórico de la Polimerización de Etileno Catalizada por Catión Metil-Bis(ciclopentadienil)Metaloceno del Grupo IVB*; PhD thesis; Pontificia Universidad Católica de Chile, June 2008.

(13) Das, P. K.; Dockter, D. W.; Fahey, D. R.; Lauffer, D. E.; Hawkins, G. D.; Li, J.; Zhu, T.; Cramer, C. J.; Truhlar, D. G.; Dapprich, S.; Froese, R. D. J.; Holthausen, M. C.; Liu, Z.; Mogi, K.; Vyboishchikov, S.; Musaev, D. G.; Morokuma, K. *Ethylene Polymerization by Zirconocene Catalysis*; Research Report for Supercomputing Institute for Digital Simulation and Advanced Computation, University of Minnesota, Minneapolis, MN, June 1998.

(14) Cossée, P. Ziegler-Natta Catalysis I. Mechanism of Polymerization of α-olefins with Ziegler-Natta Catalysts. *J. Catal.* **1964**, *3*, 80−88.

(15) Arlman, E. J. Ziegler-Natta Catalysis II. Surface Structure of Layer-Lattice Transition Metal Chlorides. *J. Catal.* **1964**, *3*, 89−98.

(16) Arlman, E. J.; Cossée, P. Ziegler-Natta Catalysis III. Stereospecific Polymerization of Propene with the Catalyst System TiCl₃ AlEt₃. *J. Catal.* **1964**, *3*, 99−104.

(17) Ystenes, M. The Trigger Mechanism for Polymerization of α-olefins with Ziegler-Natta Catalysts: A New Model Based on Interaction of Two Monomers at the Transition State and Monomer Activation of the Catalytic Centers. *J. Catal.* **1991**, *129*, 383−401.

(18) Ferreira, M. L. A Proposed Mechanism for Olefin Polymerization, 1. C_2v, C_2 and C_S Zirconocene Catalysts. *Macromol. Theory Simul.* **2002**, *11*, 250−266.

(19) Kaminsky, W.; Laban, A. Metallocene Catalysis. *Appl. Catal. A: Gen.* **2001**, *222*, 47−61.

(20) Pédetour, J. N.; Radhakrishnan, K.; Cramail, H.; Deffieus, A. Reactivity of Metallocene Catalysts for Olefin Polymerization: Influence of Activator Nature and Structure. *Macromol. Theory Simul.* **2001**, *22*, 1095−1123.

(21) Ferreira, M. L. A Proposed Mechanism for Olefin Polymerization, 2. EHMO and MM2 study. *Macromol. Theory Simul.* **2002**, *11*, 267−286.

(22) Sinn, H.; Kaminsky, W. Ziegler-Natta Catalysis. *Adv. Organomet. Chem.* **1980**, *18*, 99−149.

(23) Chen, E. Y.; Marks, T. J. Cocatalysts for Metal-Catalyzed Olefin Polymerization: Activators, Activation Processes, and Structure-Activity Relationships. *Chem. Rev.* **2000**, *100*, 1391−1434.

(24) Zurek, E.; Woo, T. K.; Firman, T. K.; Ziegler, T. Modeling the Dynamic Equilibrium between Oligomers of $(AlOCH_3)_n$ in Methylaluminoxane (MAO). A Theoretical Study Based on a Combined Quantum Mechanical and Statistical Mechanical Approach. *Inorg. Chem.* **2001**, *40*, 361−370.

(25) Zurek, E.; Ziegler, T. A Combined Quantum Mechanical and Statistical Mechanical Study of the Equilibrium of Trimethylaluminum (TMA) and Oligomers of $(AlOCH_3)_n$ found in Methylaluminoxane (MAO) Solution. *Inorg. Chem.* **2001**, *40*, 3279−3292.

(26) Zurek, E.; Ziegler, T. Toward the Identification of Dormant and Active Species in MAO (Methylaluminoxane)-Activated, Dimethylzirconocene-Catalyzed Olefin Polymerization. *Organometallics* **2002**, *21*, 83−92.

(27) Resconi, L.; Cavallo, L.; Fait, A.; Piemontesi, F. Selectivity in Propene Polymerization with Metallocene Catalysts. *Chem. Rev.* **2000**, *100*, 1253−1346.

(28) Alt, H. G.; Köppl, A. Effect of the Nature of Metallocene Complexes of Group IV Metals on their Performance in Catalytic Ethylene and Propylene Polymerization. *Chem. Rev.* **2000**, *100*, 1205−1222.

(29) Hohenberg, P.; Kohn, W. Inhomogeneous Electron Gas. *Phys. Rev. B* **1964**, *136*, 864−871.

(30) Kohn, W.; Sham, L. J. Self-Consistent Equations Including Exchange and Correlation Effects. *Phys. Rev. A* **1965**, *140*, 1133−1138.

(31) Chermette, H. Chemical Reactivity Indexes in Density Functional Theory. *J. Comput. Chem.* **1999**, *20*, 129−154.

(32) Geerlings, P.; De Proft, F.; Langenaeker, W. Conceptual Density Functional Theory. *Chem. Rev.* **2003**, *103*, 1793−1874.

(33) Johnson, P. A.; Bartolotti, L. J.; Ayers, P. W.; Fievez, T.; Geerlings; P. Chemical Density and Chemical Reactions: A Unified View from Conceptual DFT. In *Modern Charge-Density Analysis*; Gatti, C., Macchi, P., Eds., Springer: New York, 2012; pp 715−764.

(34) Geerlings, P.; Ayers, P. W.; Toro-Labbé, A.; Chattaraj, P. K.; De Proft, F. The Woodward-Hoffmann Rules Reinterpreted by Conceptual Density Functional Theory. *Acc. Chem. Res.* **2012**, *45*, 683−695.

(35) Geerlings, P.; De Proft, F. Conceptual DFT: The Chemical Relevance of Higher Response Functions. *Phys. Chem. Chem. Phys.* **2008**, *10*, 3028−3042.

(36) Morell, C.; Grand, A.; Toro-Labbé, A. New Dual Descriptor for Chemical Reactivity. *J. Phys. Chem. A* **2005**, *109*, 205−212.

(37) Morell, C.; Grand, A.; Toro-Labbé, A. Theoretical Support for Using the $\Delta f(\mathbf{r})$ Descriptor. *Chem. Phys. Lett.* **2006**, *425*, 342−346.

(38) Ayers, P. W.; Morell, C.; De Proft, F.; Geerlings, P. Understanding the Woodward-Hoffmann Rules by Using Changes in Electron Density. *Chem.—Eur. J.* **2007**, *13*, 8240−8247.

(39) Morell, C.; Ayers, P. W.; Grand, A.; Gutiérrez-Oliva, S.; Toro-Labbé, A. Rationalization of Diels-Alder Reactions Through the Use of the Dual Reactivity Descriptor $\Delta f(\mathbf{r})$. *Phys. Chem. Chem. Phys.* **2008**, *10*, 7239−7246.

(40) Morell, C.; Hocquet, A.; Grand, A.; Jamart-Grégoire, B. A Conceptual DFT Study of Hydrazino Peptides: Assessment of the Nucleophilicity of the Nitrogen Atoms by Means of the Dual Descriptor $\Delta f(\mathbf{r})$. *J. Mol. Struct. (THEOCHEM)* **2008**, *849*, 46−51.

(41) Cárdenas, C.; Rabi, N.; Ayers, P. W.; Morell, C.; Jaramillo, P. Chemical Reactivity Descriptors for Ambiphilic Reagents: Dual Descriptor, Local Hypersoftness, and Electrostatic Potential. *J. Phys. Chem. A* **2009**, *113*, 8660−8667.

(42) Fuentealba, P.; Parr, R. G. Higher-Order Derivatives in Density-Functional Theory, Especially the Hardness Derivative $\partial \eta / \partial$. N. *J. Chem. Phys.* **1991**, *94*, 5559−5564.

(43) Parr, R. G.; Yang, W. *Density-Functional Theory of Atoms and Molecules*; Oxford University Press: New York, 1989.

(44) Martínez-Araya, J. I. Revisiting Caffeate's Capabilities as a Complexation Agent to Silver Cation in Mining Processes by Means of the Dual Descriptor-A Conceptual DFT Approach. *J. Mol. Model.* **2012**, *18*, 4299−4307.

(45) Liu, S.; Ess, D. H.; Schauer, C. K. Density Functional Reactivity Theory Characterizes Charge Separation Propensity in Proton-Coupled Electron Transfer Reactions. *J. Phys. Chem. A* **2011**, *115*, 4738−4742.

(46) Kumar, N.; Liu, S.; Kozlowski, P. M. Charge Separation Propensity of the Coenzyme B12-Tyrosine Complex in Adenosylcobalamin-Dependent Methylmalonyl-Coa Mutase Enzyme. *J. Phys. Chem. Lett.* **2012**, *3*, 1035−1038.

(47) Flores-Moreno, R. Symmetry Conservation in Fukui Functions. *J. Chem. Theory Comput.* **2010**, *6*, 48−54.

(48) Martínez, J. Local Reactivity Descriptors From Degenerate Frontier Molecular Orbitals. *Chem. Phys. Lett.* **2009**, *478*, 310−322.

(49) Martínez, J. I.; Moncada, J. L.; Larenas, J. M. The Dual Descriptor to Measure Local Reactivity on Buckminster Fullerenes: An Analysis Within the Framework of Conceptual DFT. *J. Mol. Model.* **2010**, *16*, 1825−1832.

(50) Cárdenas, C.; Ayers, P. W.; Cedillo, A. Reactivity Indicators for Degenerate States in the Density-Functional Theoretic Chemical Reactivity Theory. *J. Chem. Phys.* **2011**, *134*, 174103.

(51) Labet, V.; Morell, C.; Grand, A.; Cadet, J.; Cimino, P.; Barone, V. Formation of Cross-Linked Adducts Between Guanine and Thymine Mediated by Hydroxyl Radical and One-Electron Oxidation: A Theoretical Study. *Org. Biomol. Chem.* **2008**, *6*, 3300−3305.

(52) Morell, C.; Grand, A.; Toro-Labbé, A.; Chermette, H. Is Hyper-Hardness more Chemically Relevant than Expected? *J. Mol. Model.* **2013**, *19*, 2893−2900.

(53) Yang, W.; Parr, R. G. Hardness, Softness, and the Fukui Function in the Electronic Theory of Metals and Catalysis. *Proc. Natl. Acad. Sci. U.S.A.* **1985**, *82*, 6723−6726.

(54) Senet, P. Nonlinear Electronic Responses, Fukui Functions and Hardnesses as Functionals of the Ground-State Electronic Density. *J. Chem. Phys.* **1996**, *105*, 6471−6489.

(55) Cardenas, C.; Echegaray, E.; Chakraborty, D.; Anderson, J. S. M.; Ayers, P. W. Relationships between the Third-Order Reactivity Indicators in Chemical Density-Functional Theory. *J. Chem. Phys.* **2009**, *130*, 244105.

(56) Koopmans, T. A. Über die Zuordnung von Wellenfunktionen und Eigenwerten zu den Einzelnen Elektronen eines Atoms. *Physica* **1933**, *1*, 104−113.

(57) Zielinski, F.; Tognetti, V.; Joubert, L. Condensed Descriptors for Reactivity: A Methodological Study. *Chem. Phys. Lett.* **2012**, *527*, 67−72.

(58) Savin, A.; Umrigar, C. J.; Gonze, X. Relationship of Kohn-Sham Eigenvalues to Excitation Energies. *Chem. Phys. Lett.* **1998**, *288*, 391−395.

(59) Ayers, P. W.; Morrison, R. C.; Parr, R. G. Fermi-Amaldi Model for Exchange-Correlation: Atomic Excitation Energies from Orbital Energy Differences. *Mol. Phys.* **2005**, *103*, 2061−2072.

(60) Schlegel, H. B. Optimization of Equilibrium Geometries and Transition Structures. *J. Comput. Chem.* **1982**, *3*, 214−218.

(61) Becke, A. D. Density-Functional Thermochemistry. III. The Role of Exact Exchange. *J. Chem. Phys.* **1993**, *98*, 5648−5652.

(62) Lee, C.; Yang, W.; Parr, R. G. Development of the Colle-Salvetti Correlation-Energy Formula into a Functional of the Electron Density. *Phys. Rev. B* **1988**, *37*, 785−789.

(63) Miehlich, B.; Savin, A.; Stoll, H.; Preuss, H. Results Obtained with the Correlation Energy Density Functionals of Becke and Lee, Yang and Parr. *Chem. Phys. Lett.* **1989**, *157*, 200−206.

(64) Vosko, S. H.; Wilk, L.; Nusair, M. Accurate Spin-Dependent Electron Liquid Correlation Energies for Local Spin Density Calculations: A Critical Analysis. *Can. J. Phys.* **1981**, *58*, 1200−1211.

(65) Hariharan, P. C.; Pople, J. A. The Influence of Polarization Functions on Molecular Orbital Hydrogenation Energies. *Theor. Chim. Acta* **1973**, *28*, 213−222.

(66) Frisch, M. J.; Pople, J. A.; Binkley, J. S. Self-Consistent Molecular Orbital Methods 25. Supplementary Functions for Gaussian Basis Sets. *J. Chem. Phys.* **1984**, *80*, 3265−3269.

(67) Hay, P. J.; Wadt, W. R. Ab Initio Effective Core Potentials for Molecular Calculations. Potentials for the Transition Metal Atoms Sc to Hg. *J. Chem. Phys.* **1985**, *82*, 270−283.

(68) Wadt, W. R.; Hay, P. J. Ab Initio Effective Core Potentials for Molecular Calculations. Potentials for Main Group Elements Na to Bi. *J. Chem. Phys.* **1985**, *82*, 283−298.

(69) Hay, P. J.; Wadt, W. R. Ab Initio Effective Core Potentials for Molecular Calculations. Potentials for K to Au Including the Outermost Core Orbitals. *J. Chem. Phys.* **1985**, *82*, 299−310.

(70) Frisch, M. J. et al. *Gaussian 09*, revision B.01; Gaussian Inc.; Wallingford CT, 2009.

(71) Contreras, R. R.; Fuentealba, P.; Galván, M.; Pérez, P. A Direct Evaluation of Regional Fukui Functions in Molecules. *Chem. Phys. Lett.* **1999**, *304*, 405−413.

(72) Fuentealba, P.; Pérez, P.; Contreras, R. On the Condensed Fukui Function. *J. Chem. Phys.* **2000**, *113*, 2544−2551.

(73) Chamorro, E. Fukui, rev 1.1, 2011.

(74) Chamorro, E.; Pérez, P. Condensed-to-Atoms Electronic Fukui Functions within the Framework of Spin-Polarized Density-Functional Theory. *J. Chem. Phys.* **2005**, *123*, 114107.

(75) Liu, S. Steric Effect: A Quantitative Description from Density Functional Theory. *J. Chem. Phys.* **2007**, *126*, 244103.

(76) Liu, S.; Govind, N. Toward Understanding the Nature of Internal Rotation Barriers with a New Energy Partition Scheme: Ethane and n-Butane. *J. Phys. Chem. A* **2008**, *112*, 6690−6699.

(77) Tsirelson, V. G.; Stash, A. I.; Liu, S. Quantifying Steric Effect with Experimental Electron Density. *J. Chem. Phys.* **2010**, *133*, 114110.

(78) Esquivel, R. O.; Liu, S.; Angulo, J. C.; Dehesa, J. S.; Antolín, J.; Molina-Espíritu, M. Fisher Information and Steric Effect: Study of the Internal Rotation Barrier of Ethane. *J. Phys. Chem. A* **2011**, *115*, 4406−4415.

(79) Huang, Y.; Zhong, A. G.; Yang, Q.; Liu, S. Origin of Anomeric Effect: A Density Functional Steric Analysis. *J. Chem. Phys.* **2011**, *134*, 084103.

(80) Ess, D. H.; Liu, S.; De Proft, F. Density Functional Steric Analysis of Linear and Branched Alkanes. *J. Phys. Chem. A* **2010**, *114*, 1295−12957.

(81) Torrent-Sucarrat, M.; Liu, S.; De Proft, F. Steric Effect: Partitioning in Atomic and Functional Group Contributions. *J. Phys. Chem. A* **2009**, *113*, 3698−3702.